Applied Energy 222 (2018) 396–409

Contents lists available at ScienceDirect

Applied Energy

journal homepage: www.elsevier.com/locate/apenergy

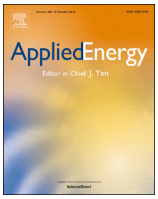

Optimization and multi-time scale modeling of pilot solar driven polygeneration system based on organic Rankine cycle

Ying Zhang, Shuai Deng, Li Zhao*, Shan Lin, Jiaxin Ni, Minglu Ma, Weicong Xu

Key Laboratory of Efficient Utilization of Low and Medium Grade Energy (Tianjin University), MOE, Tianjin 300072, China

HIGHLIGHTS

- The field test of pilot distributed solar driven ORC-based CCHP system is presented.
- A multi-time scale simulation mechanism is developed.
- The objective and functionality of each time-scale simulation with appropriate time step is identified.
- A model-guided optimized system is achieved with sequential configuration.

ARTICLE INFO

Keywords:
Combined cooling, heating, and power
Organic Rankine cycle
Pilot system
Solar thermal energy
Simulation
Time scale

ABSTRACT

Pilot-scale distributed polygeneration system driven by solar energy and its effective simulation mechanism provides promising solutions for the technology promotion and implementation, as the emerging of smart grid concepts. In this regard, this study aims to preliminary test such a system based on organic Rankine cycle with the power output of 200 kW, which is combined with cooling and heating cycle. The developed pilot system is proven to sustain the power thermal efficiency of 10% with R123 and a self-made expansion valve. Targeting a whole optimized system in practical application, a multi-time scale mechanism is proposed and consists of long-, mid- and short-term simulation with yearly, hourly and second time step, respectively. The functionality of the concept is proven by showing the model-guided optimal sequential system with hexamethyldisiloxane working fluid. It achieves a high performance ratio, efficient cost, and less land occupation, corresponding to 67.61%, \$0.12 million and 3774.2 m^2, respectively, under the long-term simulation. Rated operation decisions are correspondingly determined and present acceptable supply-and-demand matching performance at the level of mid-term modeling, with the payback time of 7.41 years. Furthermore, the system dynamic behavior is analyzed in two typical sunny and cloudy days to understand and compare its running states. The short-term model shows a steady thermal efficiency of 9.6% within 15,000 s and capture a smaller period of safety state only within 6000 s under the sunny day condition. Although the peak irradiance in the cloudy day is higher than that in the sunny day, the performance degrades dramatically due to the irradiance fluctuation. It is expected that the proposed mechanism can be extended in analyzing operational security and control strategy.

1. Introduction

Due to the increasing global demand for energy, as well as the strict emissions targets, popularization and application of renewable energy systems is an urgent goal for all over the world to pursue. According to Renewable Energy Policy Network for the 21st Century, new investment in renewable energy from 2015 to 2016 continued to be dominated by solar, which accounted for roughly 47% of total investments in 2016 [1]. Its strong growth gave a clear indication of accounting for all of the increase in global renewable energy penetration, with solar technology as the backbone of the highly decarbonized energy system. China proposes an ambitious renewable penetration objective in 2050 with over 60% of China's total energy consumption and with 2700 GW solar units [2]. To access this goal, a first batch of concentrated solar power (CSP) demonstration projects have been officially released with an installed capacity of 1.35 GW, constituting 64% among the total CSP in the world. However, these projects locate in the sparsely populated western region of China with rich radiation resources, and commonly belong to centralized power generation system.

As the emerging of smart grid concept, societal-scale infrastructures such as eco-industrial parks [3] and smart buildings are rapidly expanded [4]. For such infrastructures, diversification of energy products

---

* Corresponding author.
E-mail address: jons@tju.edu.cn (L. Zhao).

https://doi.org/10.1016/j.apenergy.2018.03.118
Received 31 December 2017; Received in revised form 11 March 2018; Accepted 27 March 2018

Nomenclature

Acronyms

ACH	absorption chiller
CCP	combined cooling and heating
CCHP	combined cooling, heating and power
CHP	combined cooling and heating
Cond_ORC	condenser
CPC	compound parabolic collector
ETC	evacuated tube collector
HS	heating storage
e-CPS	energy-cyber-physical
ICE	internal-combustion engine
NPV	net present value
PTC	parabolic trough collector
PBT	payback time
P_Oil	oil pump
P_ORC	working fluid pump
PS	parallel system
SS	sequential system
VG	vapor generator
WHR	waste heat recovery

Symbols

A	area, m^2
A_i	circumferential area of segment “i”, m^2
a	coefficient, –
b	coefficient, –
c	specific heat capacity, J/kg
C_g	geometric concentration ratio, –
cor	corrected, –
D	diameter, m
d_i	inner diameter of tubes, m
d_o	outer diameter of tubes, m
des	design condition
E	total energy in volume, J
F	objective, –
F_e	dirt degree of collector’s mirrors, –
FF	filling factor, –
G_{b}	solar irradiance, W/m^2
GT	gas turbine
$g(t)$	generated energy, kWh
h	specific enthalpy, J/kg
h_i	specific enthalpy of fluid in each heat exchanger segment, J/kg
hr	hour, –
i	the number of points on the Pareto frontier, –
I_{b}	hourly solar beam radiation, W/m^2
IC	investment cost, $
K	incident angle modifier, –
k	the order of each variable
$l(t)$	load, kWh
M	total mass in volume, kg
M_i	the mass of fluid in each heat exchanger segment, kg
$\dot{m}$	mass flow rate, kg/s
N	the number of segments.
n	rotate speed, –
N_{rot}	rotating speed, rpm
P	pressure, Pa
p	the index for each point on the Pareto front, –
PR	overall efficiency of solar energy, –
$\dot{Q}$	heat power, W
$\bar{\dot{Q}}_i$	heat power of fluid in each segment, W
q	the index for each objective, –
$\dot{q}_i''$	net heat flux per unit area, W/m^2
R_k	net cash inflow during period k, $
R	coefficient, –
$S(t)$	energy storage balance, kWh
t	time, s
T	temperature, ^{o}C
$\bar{T}$	average temperature
ΔT	temperature difference, ^{o}C
U	internal energy, J
U_0	overall heat transfer coefficient, W/m^2.^{o}C
U_L^{abs}	thermal loss coefficient of absorber, –
v	specific volume, m^3/kg
v_{bf}	bulk fluid velocity, m/s
V	volume, m^3
$\dot{V}$	volumetric flow, m^3/s
$\dot{W}$	power, kW
x	axial distance, m

Greek symbols

α	heating price and electricity price ratio
β	cooling price and electricity price ratio
ε	effectiveness
$\varepsilon_{\mathrm{over,pp}}$	pump internal isentropic efficiency
η	efficiency
ρ	density, kg/m^3
$\bar{\rho}_i$	fluid density of fluid in each heat exchanger segments, kg/m^3
φ	incident angle, –
ϕ	level fraction
Δ	difference
λ	thermal conductivity
γ	load cover factor

Subscripts

a	aperture of PTC
abs	absorber of PTC
cd	condenser
em	electromechanical
exp	expender
ex	exhaust or outlet
eva	evaporator
f	fluid
HE	heat exchanger
heat_sur	surplus heat from condenser
hf	hot fluid
hs	heat source
i	inside fluid of HE
id	inside dirt of HE
in	internal
inc	state energy incentives
l	liquid
lm	logarithm mean
max	the maximum
mech	mechanical
net	gross mechanical output
opt,0^{o}	collector’s optical efficiency for zero incident angle
o	outside fluid of HE
od	outside dirt
pin	pinch point
pp	pump
ref	reference
s	swept